Seizures, sensorineural deafness, ataxia, mental retardation, and electrolyte imbalance (SeSAME syndrome) caused by mutations in *KCNJ10*

Ute I. Scholl[a], Murim Choi[a], Tiewen Liu[a], Vincent T. Ramaekers[b], Martin G. Häusler[c], Joanne Grimmer[d,1], Sheldon W. Tobe[e], Anita Farhi[a], Carol Nelson-Williams[a], and Richard P. Lifton[a,2]

[a]Department of Genetics, The Howard Hughes Medical Institute, Yale University School of Medicine, 333 Cedar Street, New Haven, CT 06510; [b]Department of Paediatrics, Centre Hospitalier Universitaire, Domaine Universitaire du Sart Tilman, Bâtiment B 35, B-4000 Liège 1, Belgium; [c]Department of Paediatrics, University Hospital, RWTH Aachen, Pauwelsstrasse 30, 52074 Aachen, Germany; [d]Department of Nephrology, The Hospital for Sick Children, 555 University Avenue, Toronto, ON, Canada M5G 1X8; and [e]Division of Nephrology, Sunnybrook Health Sciences Centre, 2075 Bayview Avenue, Toronto, ON, Canada M4N 3M5

Contributed by Richard P. Lifton, February 18, 2009 (sent for review January 29, 2009)

We describe members of 4 kindreds with a previously unrecognized syndrome characterized by seizures, sensorineural deafness, ataxia, mental retardation, and electrolyte imbalance (hypokalemia, metabolic alkalosis, and hypomagnesemia). By analysis of linkage we localize the putative causative gene to a 2.5-Mb segment of chromosome 1q23.2–23.3. Direct DNA sequencing of *KCNJ10*, which encodes an inwardly rectifying K^+ channel, identifies previously unidentified missense or nonsense mutations on both alleles in all affected subjects. These mutations alter highly conserved amino acids and are absent among control chromosomes. Many of these mutations have been shown to cause loss of function in related K^+ channels. These findings demonstrate that loss-of-function mutations in *KCNJ10* cause this syndrome, which we name SeSAME. *KCNJ10* is expressed in glia in the brain and spinal cord, where it is believed to take up K^+ released by neuronal repolarization, in cochlea, where it is involved in the generation of endolymph, and on the basolateral membrane in the distal nephron. We propose that *KCNJ10* is required in the kidney for normal salt reabsorption in the distal convoluted tubule because of the need for K^+ recycling across the basolateral membrane to enable normal activity of the Na^+-K^+-ATPase; loss of this function accounts for the observed electrolyte defects. Mice deficient for *KCNJ10* show a related phenotype with seizures, ataxia, and hearing loss, further supporting *KCNJ10*'s role in this syndrome. These findings define a unique human syndrome, and establish the essential role of basolateral K^+ channels in renal electrolyte homeostasis.

Gitelman syndrome | hypokalemia | hypomagnesemia | inwardly rectifying K^+ channel | renal salt wasting

Transmembrane ion flux via channels, transporters, and pumps plays a critical role in diverse physiologic functions, including neuronal signal transmission and electrolyte and volume homeostasis. In many cases, homologous electrolyte flux processes in different tissues are mediated by the encoded products of distinct genes, while in a few cases the identical gene products are involved. Evidence of the latter comes from Mendelian diseases in which mutation in a single gene produces effects on both auditory and renal function. For example, loss-of-function mutations in *ATP6B1*, which encodes a subunit of the H^+-ATPase, result in systemic acidosis because of a renal defect in H^+ secretion and sensorineural hearing loss caused by defective H^+ secretion into the cochlear endolymph, resulting in impaired hair cell function and deafness (1). Similarly, mutations in barttin, which encodes a subunit of the CLCNKA and CLCNKB chloride channels, result in renal salt wasting and deafness (2).

The genetic dissection of renal diseases featuring low serum potassium (hypokalemia) and metabolic alkalosis (high serum pH) has identified many components required for normal renal electrolyte homeostasis (2–7). In all cases, this syndrome has resulted from increased activity of the epithelial Na^+ channel (ENaC) on the apical membrane, which leads to increased secretion of K^+ and H^+ because of the more negative luminal potential. Hypokalemia with alkalosis can result either from primary increases in ENaC activity because of mutations in ENaC itself (3), or from activation of ENaC by aldosterone in response to reduced intravascular volume (7). Mutations that cause impaired salt reabsorption in the thick ascending limb of Henle or the distal convoluted tubule cause salt wasting that leads to secondary increases in ENaC activity and hypokalemic alkalosis. Identified mutations in these diseases, referred to as Bartter and Gitelman syndromes, are in genes including 2 apical Na^+-Cl^- transporters that mediate Na-Cl entry into epithelia, 2 Cl^- channel subunits that mediate exit of Cl^- across the basolateral membrane, and an apical K^+ channel (2, 4–7). These syndromes are distinguished clinically by marked hypomagnesemia and low urinary calcium in Gitelman syndrome, while hypercalciuria with normal or modest reductions in Mg^{2+} is observed in Bartter syndrome.

Similarly, a number of Mendelian seizure disorders have been described. Many of these result from mutations that depolarize neurons, increasing neuronal excitability and reducing seizure threshold. Examples include benign familial neonatal seizures caused by mutations in the *KCNQ2/3* K^+ channels (8, 9), benign familial neonatal/infantile seizures caused by mutations in the *SCN2A* gene encoding the alpha subunit of voltage gated Na^+ channels (10), and several idiopathic epilepsy syndromes caused by mutations in the *SCN1A* sodium channel (11).

Considering the many similarities in the mechanisms governing renal electrolyte homeostasis and neuronal function, it is surprising that relatively few single-gene disorders that have effects on both have been identified. Here, we describe a previously unrecognized complex syndrome featuring seizures, sensorineural deafness, ataxia, mental retardation and electrolyte imbalance (SeSAME), and demonstrate that it is caused by mutation in *KCNJ10*, which encodes a K^+ channel expressed in epithelia of the kidney and inner ear, as well as glial cells in the CNS.

Author contributions: U.I.S., M.C., and R.P.L. designed research; U.I.S., M.C., T.L., V.T.R., M.G.H., J.G., S.W.T., A.F., C.N.-W., and R.P.L. performed research; U.I.S., M.C., T.L., and R.P.L. analyzed data; and U.I.S., M.C., and R.P.L. wrote the paper.

The authors declare no conflict of interest.

Freely available online through the PNAS open access option.

[1]Present address: Department of Paediatrics, University of Western Ontario, 800 Commissioners Road East, London, Ontario, Canada N6A 5W9.

[2]To whom correspondence should be addressed. E-mail: richard.lifton@yale.edu.

Table 1. Clinical features of affected patients

Clinical feature	Patient number				
	327–1	404–1	441–1	632–1	632–2
Ancestry	Great Britain	Turkey	Afghanistan	Canada	Canada
Consanguinity	N/A	Yes	Yes	No	No
Seizures (age of onset in months)	+ (N/A)	+ (4)	+ (3)	+ (3)	+ (3)
Ataxia	+	+	+	+	+
Developmental delay	+	+	+	+	+
Hearing loss	+	+	+	+	+
K^+ (mmol/l)	2.9	3.15	3.1	3.1	2.9
Mg^{2+} (mmol/l)	0.55	0.62	0.54	0.56	0.6
HCO_3^- (mmol/l)	28	30	29	31	33
U_{Ca}/U_{Cr} (mmol/mmol)	0.11	0.34	0.10	N/A	0.26
U_K/U_{Cr} (mmol/mmol)	38.18	24.28	21.67	N/A	16.18
U_{Na}/U_{Cr} (mmol/mmol)	19.09	25.86	32.50	N/A	23.86

K^+, serum potassium, nl 3.5–5 mmol/l; Mg^{2+}, serum magnesium, nl 0.8–1.2 mmol/l; HCO_3^-, serum bicarbonate, nl 23–26 mmol/l; U_{Ca}/U_{Cr}, urinary calcium/creatinine ratio, nl $<$ 0.4 mmol/mmol); U_K/U_{Cr}, urinary potasssium/creatinine ratio [nl 6–8 mmol/mmol, or 1–1.5 mmol/mmol in hypokalemia (36)]; U_{Na}/U_{Cr}, urinary sodium/creatinine ratio, values are elevated and in the range observed in patients with Gitelman syndrome (30).

Results

Case Report: Kindred 441. The index case, patient 441–1, is a 24-year-old female of Afghan ancestry who is the fifth of 6 offspring of healthy first-cousins. Generalized seizures began at 3 months, occurring several times daily. Seizures were controlled initially with phenobarbital, and later diphenylhydantoin. Sitting was first demonstrated at age 1 year, crawling at age 20 months.

At age 5 years 7 months, the patient presented for evaluation of developmental delay. At this time, she was unable to walk or speak. Physical examination was notable for atrophy of the lower extremities without contractures. Motor strength was slightly reduced in the upper, but markedly reduced in the lower extremities. Reflexes were normal. There was marked ataxia. Nerve conduction studies revealed reduced conduction velocity in the left peroneal and left tibial nerves (36 and 37 m/sec, respectively; nl 40–44 m/sec). A muscle and nerve biopsy showed normal muscle other than fiber-type disproportion; there was hypomyelination of the large myelinated nerve fibers in the sural nerve, with moderate progressive axonal neuropathy. Brain MRI showed normal myelination, and was normal with the exception of slightly coarsened frontal sulci. EEG, abdominal ultrasound, and karyotype analysis were normal.

Laboratory evaluation was remarkable for persistent hypokalemia, metabolic alkalosis, and hypomagnesemia (Table 1). Plasma renin activity (PRA) was elevated on repeated measures (8.1 and 7.6 ng/ml per hour, nl $<$2.8 ng/ml per hour). Twenty-four-hour urinary aldosterone level was elevated (31.3 μg; nl 5.9–17.6) and the Ca^{2+}/creatinine ratio was low (0.1 to 0.2 mmol/mmol). The patient was treated with oral potassium replacement, and required 30 meq per day to maintain a K^+ level in the normal range. At age 18, progressive hearing loss was noted. Brainstem-evoked response audiometry and pure-tone threshold audiometry were performed, and moderate-to-severe sensorineural hearing loss was documented.

The patient's family history is notable for 2 of 5 siblings with a related disorder, and one spontaneous abortion. The first child, a male, presented with seizures at age 4 months and was never able to walk. He died at age 7 years during a diarrheal illness. The sixth child, a male, presented with seizures and vomiting at age 5 months and was unable to walk until 16 months. He died at 18 months during an intercurrent infection. The other 3 children are healthy.

Definition of a New Clinical Syndrome. In the review of 589 subjects referred for evaluation of Gitelman and Bartter syndromes, we recognized subjects from 3 additional kindreds with features similar to patient 441–1. The shared features included early onset seizures, mental retardation, ataxia, hypotonia, and sensorineural hearing loss. Intention tremor was noted in several cases and volume loss of the cerebellum in 2 cases (632–2 and 404–1). Short stature was notable in 2 affected siblings (632–1 and 632–2), with a final height of 150 cm and 149 cm, respectively. Electrolyte abnormalities featured marked and persistent hypokalemic metabolic alkalosis in the absence of hypertension and striking hypomagnesemia that required electrolyte replacement and, in many cases, use of pharmacologic inhibitors of the epithelial sodium channel or aldosterone antagonists to prevent renal K^+ loss. Where available, 24-h urinary electrolyte measurements revealed renal K^+ and Mg^{2+} wasting and high urinary Na^+ levels. PRA and aldosterone levels, when measured, were always elevated, and salt craving, enuresis, and polyuria/polydipsia were reported. A summary of the patients' clinical and laboratory findings is provided in Table 1.

Mapping the Disease Locus. The recurrent clinical features suggested a previously unrecognized clinical syndrome. Moreover, recurrence of a similar syndrome among siblings in 2 of these kindreds, and its occurrence in the setting of parental consanguinity in 2 kindreds, suggested autosomal recessive transmission. To attempt to map the underlying disease locus, we performed genome-wide analysis of linkage in the 3 informative kindreds (2 offspring of first-cousin marriage and 2 affected siblings from unrelated parents). The results demonstrated complete linkage of the putative trait locus to a single chromosome segment, 1q23.2-q23.3, with a lod score of 3.0. The maximum likelihood location is confined to a 2.5-Mb interval extending from 158.1 M to 160.6 M base pairs (Fig. 1*A*). No other chromosome segment showed linkage in all 3 kindreds. Significantly, the index case (441–1) did not show homozygosity at any of the known loci for Bartter or Gitelman syndrome, and sequencing of these genes revealed no evidence of pathogenic mutations.

Mutations in *KCNJ10*. The linked interval on chromosome 1 contains 70 well-defined and at least 6 hypothetical genes, none of which has previously been implicated in human disease phenotypes that would explain the features found in these patients. If the disease is caused by mutation in a single gene, we anticipate that it would likely be expressed in the CNS, inner ear, and kidney. We considered ion channels, transporters, and

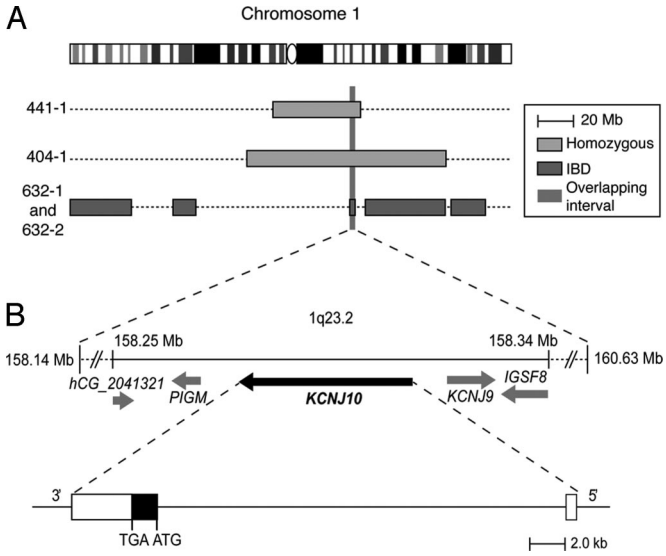

Fig. 1. Mapping the disease locus. (*A*) An ideogram of chromosome 1 is shown, with homozygous regions in patient 441–1 and 404–1 indicated by light gray boxes, and segments that are identical by descent (IBD) in the siblings 632–1 and 632–2 marked by dark gray boxes. The overlap of these intervals is marked, and represents the maximum likelihood location of the disease locus on chromosome 1q23.2-q23.3, a 4-cM interval covering 2.5 Mb from 158.1 M to 160.6 M base pairs. (*B*) The candidate interval contains *KCNJ10* on chromosome 1q23.2. Neighbouring genes are represented by arrows in their corresponding transcriptional orientations. *KCNJ10* comprises 2 exons indicated by boxes, with the coding sequence indicated in black.

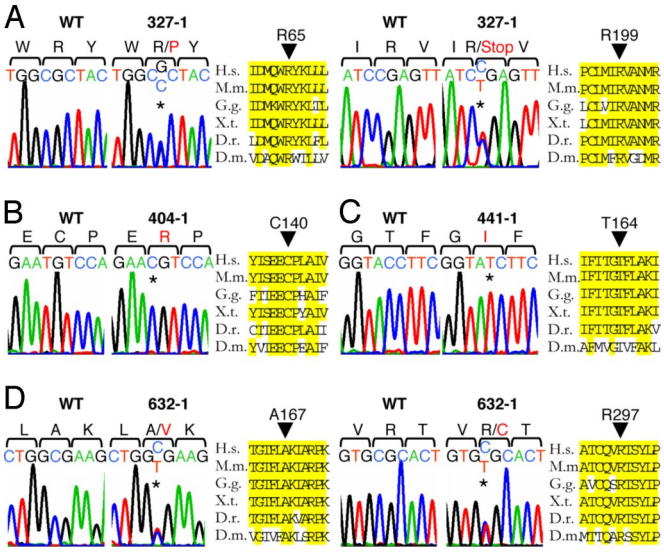

Fig. 2. Mutations in *KCNJ10* in affected patients. In each panel the DNA sequences of the sense strand of wild-type subjects (*Left*) and affected subjects (*Right*) are shown. The sequence of the encoded peptide is indicated in single letter code. A ClustalW alignment of the *Homo sapiens* (H.s.) protein sequence with orthologs and paralogs from *Mus musculus* (M.m.), *Gallus gallus* (G.g.), *Xenopus tropicalis* (X.t.), *Danio rerio* (D.r.), and *Drosophila melanogaster* (D.m.) is shown next to each mutation. The human sequence and residues conserved in orthologs and paralogs are marked in yellow, and the mutant residue is indicated. (*A*) Patient 327–1 is compound heterozygous for a missense and a nonsense mutation in *KCNJ10*. (*B*) Patient 404–1 is homozygous for a missense mutation, changing codon TGT (C140) to CGT (R140). (*C*) A homozygous missense mutation was found in kindred 441, resulting in change of codon ACC (T164) to ATC (I164). (*D*) In kindred 632, both affected siblings are compound heterozygous for missense mutations: A167V and R297C.

regulators of their function to be leading candidates. We identified *KCNJ10*, which encodes the inwardly rectifying K^+ channel Kir4.1 (also known as BIR10, BIRK1, K_{AB}-2, Kir1.2), consisting of 2 transmembrane segments and 1 pore, as a strong candidate (Fig. 1*B*). *KCNJ10* has been shown to be expressed in the CNS, cochlea, and distal nephron, and a mouse knockout has a neurological phenotype with many features similar to those seen in our patients (see *Discussion*).

We screened available members of the 4 kindreds with this syndrome for *KCNJ10* mutations by direct sequencing (Fig. 2). We found homozygous missense mutations in the 2 consanguineous kindreds, compound heterozygous missense mutations in 1 outbred kindred, and a compound missense/premature termination mutation in 1 kindred. In the compound heterozygous patients, cloning of the coding region on single amplicons confirmed that the 2 mutations identified are in *trans*. To assess the significance of missense mutations, we compared the *KCNJ10* amino acid sequence to orthologs in diverse vertebrate species including mammals, *Xenopus tropicalis*, and zebrafish, and closely related paralogs in chicken and *Drosophila melanogaster* (see *Methods*). These species split from a common ancestor ≈500 million years ago, and across these species, only 27% of the amino acids were completely conserved. All of the identified mutations occurred at positions that were completely conserved among all vertebrate species and all but one occurred at positions completely conserved through *Drosophila* (see Fig. 2).

Patient 327–1 was compound heterozygous for a nonsense and a missense mutation (see Fig. 2*A*). The nonsense mutation introduces a premature termination codon at position 199 in the cytoplasmic C terminus. This deletes a PDZ-binding domain that is known to be required for expression of Kir4.1 at the cell surface (12). This patient also harbors an R65P substitution immediately preceding the first transmembrane domain (Fig. 3). This position is conserved in a related inward rectifier, Kir2.1, and expression of Kir2.1 containing mutation at this position abolished nearly all detectable whole-cell K^+ current when expressed in *Xenopus* oocytes (13).

Affected subject 404–1 was homozygous for a C140R missense mutation (see Fig. 2*B*). C140 is located in the P region near the start of the second transmembrane domain (see Fig. 3). This position is conserved in the related channel ROMK (position C153), and mutation of this residue to either alanine or serine has been shown to abolish ROMK function (14).

A missense mutation was found in kindred 441, resulting in a T164I substitution (see Fig. 2*C*). The index case is homozygous for the mutant allele, while both parents are heterozygotes and

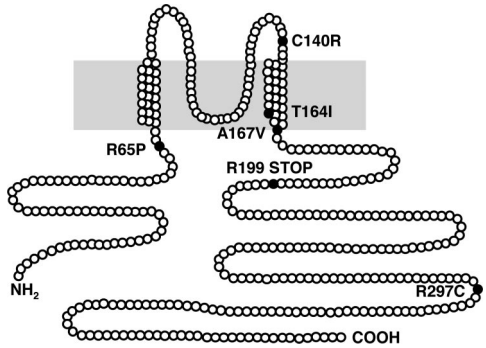

Fig. 3. Location of *KCNJ10* mutations in patients with SeSAME syndrome. A schematic view of the protein is shown, with intracellular N- and C-termini, 2 transmembrane helices (plasma membrane shown in shaded gray), and 1 pore. This structure is characteristic of the inward rectifier family. Locations of mutations are indicated by black circles, and the respective amino acid change is noted.

neither of 2 unaffected siblings are homozygous, providing further support for linkage (total lod score for linkage after inclusion of the 2 unaffected siblings increases to 3.25). Rapedius et al. (15) have suggested that T164, which is located in the second transmembrane domain, forms an intra-subunit H-bond with lysine 67 in the first transmembrane domain, and that this interaction is critical for gating of the channel. Because this lysine is predicted to form an H-bond not only with the backbone carbonyl of Thr-164, but also with its side chain oxygen, mutation to isoleucine would eliminate this interaction and potentially affect the gating properties of the channel in response to pH and phosphatidylinositol 4,5-bisphosphate (PIP_2) (see *Discussion*).

Finally, in kindred 632, both affected siblings are compound heterozygotes for A167V and R297C mutations (see Fig. 2*D*). A167 is located at the end of the second transmembrane domain, close to the constriction at the inner helix bundle that likely corresponds to the gate of the channel (16). R297 lies in a highly conserved segment in the C terminus of the protein (see Fig. 3). Notably, a mutation at the residue corresponding to R297 has been found in ROMK (R292W), and was implicated as a loss of function mutation in Bartter's syndrome type II (17). Similarly, mutation of the conserved position in Kir2.1 (R312) to glutamine greatly reduces whole-cell currents and produces weakened interaction with PIP_2 (see *Discussion*) (13).

None of the identified mutations are in the dbSNP database. Resequencing of *KCNJ10* in 103 unrelated Caucasian subjects did not identify any of these mutations and no missense variants at conserved residues were identified in any of the 206 alleles studied.

Discussion

We have defined a previously unrecognized human syndrome featuring prominent neurological and renal features and have demonstrated that in all 4 kindreds studied the disease cosegregates with rare mutations in *KCNJ10*. The finding of 6 independent rare *KCNJ10* mutations in 4 families that significantly cosegregate with the disease under a recessive model and which show specificity for the disease provides genetic evidence that these mutations are the cause of this syndrome. The fact that many of the amino acids altered by mutations are conserved in other members of the inward rectifier K^+ channel family and have been shown to be essential for their normal function lends strong support for the functional significance of these mutations. The genetic and biochemical evidence support these mutations being a genetic loss of function.

Several of the identified mutations are likely to affect channel activity via altered interaction with PIP_2. Numerous functional studies in closely related inward rectifier potassium channels have underlined the crucial role of PIP_2 to sustain activity of these channels (13). PIP_2 is a membrane-delimited second messenger, and binds proteins through electrostatic interactions at basic amino acids. These sites have been defined in many members of this gene family, and mutations at PIP_2 binding sites have been implicated in other channelopathies, including Bartter's syndrome, caused by ROMK mutations, and Andersen's syndrome, caused by mutations in *KCNJ2* encoding Kir2.1. A similar mechanism likely accounts for loss of function in at least 2 of the mutations identified here (R65P and R297C), which lie at inferred PIP_2 binding sites. A third residue (T164) has been implicated in an H-bond between the 2 transmembrane helices, which again plays an important role in the channel's gating in response to PIP_2 and pH (15).

Significant prior work has been done on *KCNJ10*; it appears to function as a heteromultimer at least in some tissues. The currents observed in native tissues have properties most similar to those produced by coexpression of Kir4.1 and Kir5.1 in heterologous systems, and immunofluorescence studies support colocalization of these gene products (18, 19). This observation raises the question of whether a related syndrome might be caused by mutation in Kir5.1.

In addition, mice with both constitutional and selective astrocyte knockout of *KCNJ10* have been produced, with a resultant phenotype that is strikingly similar to the patients we describe (20–22). The animals develop motor coordination deficits with awkward and jerky movements and loss of balance, and drag the hind limbs. They also suffer seizures and have sensorineural hearing loss (20, 23). Additionally, mice with the constitutional knockout appear to have a salt-wasting phenotype; however, this has not been well defined. These findings strongly support the mutations we identify as being loss of function.

In the brain, *KCNJ10* appears to be primarily expressed in glial cells (24), specifically in astrocytes surrounding synapses and blood vessels, and oligodendrocyte cell bodies (20). Neuronal repolarization after excitatory stimuli is achieved via efflux of K^+, and it has been proposed that *KCNJ10* plays a role in astrocyte clearance of this K^+ via "spatial buffering." If the resting membrane potential is set by KCNJ10, a local increase in extracellular K^+ concentration close to the synapse would favor K^+ uptake by astrocytes, and efflux at remote positions that have lower extracellular K^+ concentrations (i.e., the rise in extracellular K^+ would cause the local glial E_K to be less negative than the aggregate cellular membrane potential). Loss of *KCNJ10* would thus result in astrocyte depolarization [which is seen in astrocytes from *KCNJ10*-deficient mice (20)], loss of this K^+ clearance function, prolonged neuronal depolarization, and reduced seizure threshold. Similarly, astrocyte depolarization would reduce clearance of the excitatory neurotransmitter glutamate, which would also reduce seizure threshold [reduced glutamate uptake is also seen in astrocytes from *KCNJ10*-deficient mice (20)]. While other mechanisms (activities of the Na^+-K^+-ATPase or Na-K-Cl cotransporters) are also potentially involved in the regulation of synaptic K^+ (25), the observed seizure activity in humans deficient for *KCNJ10* indicates an important role of this channel in prevention of seizure activity. Finally, it is of interest that common variation in the *KCNJ10* gene has been suggested to be associated with seizure susceptibility (26), however, the functional significance of the implicated variants and the replicability of this finding has not been established.

Kir4.1 is expressed in intermediate cells of the stria vascularis (27), where it is believed to contribute to the generation of the endocochlear potential, as demonstrated by hearing loss in the *KCNJ10*-knockout mouse (23) and the patients described herein.

Both mice and humans with *KCNJ10* mutations have marked ataxia and there is also lower extremity weakness in the mouse and some affected humans. Whether the ataxia is cerebellar in origin or sensory (due to loss of proprioception) has not been established and is hard to assess because of cognitive impairment of affected subjects. Intention tremor and volume loss in the cerebellum, as seen in some cases, suggest cerebellar involvement. However, peripheral sensory neuropathy might also contribute to the ataxia.

KCNJ10-deficient mice exhibit striking pathology of the spinal cord with dysmyelination, hypomyelination, and axonal degeneration along with massive spongiform vacuolation. MRI demonstrates marked white-matter pathology in the spinal cord and brainstem, while cerebellum, midbrain, and cortical regions seem unaffected at P12. It thus appears that Kir4.1 is required for oligodendrocyte development, and at least spinal cord myelination (22). The observation that sural nerve biopsy in one of our patients showed hypomyelination suggests a possible role for *KCNJ10* in the peripheral nervous system as well, and Kir4.1 has been shown to be expressed in satellite cells (28).

The distinct electrolyte abnormalities in our patients add considerable new insight into the role of *KCNJ10* in renal electrolyte homeostasis. The *KCNJ10* gene product has been

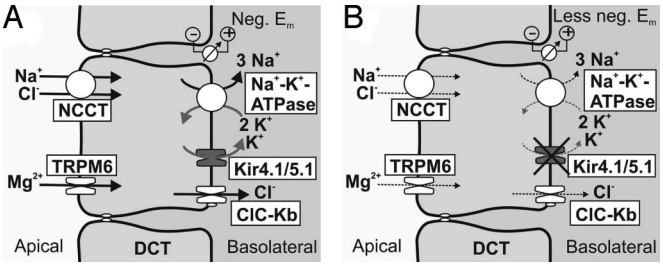

Fig. 4. A model of impaired ion transport in the distal convoluted tubule caused by mutations in the Kir4.1 inwardly rectifying potassium channel. (*A*) Kir4.1/5.1 heteromultimers in the basolateral membrane of the distal convoluted tubule (DCT) recycle potassium entering the cell via the Na^+-K^+-ATPase back into the interstitial space and contribute to the negative membrane potential that promotes basolateral chloride exit. On the luminal surface, sodium and potassium enter the cell via the thiazide sensitive cotransporter NCCT, and Mg^{2+} enters via TrpM6, using the favorable electrical gradient. (*B*) Disruption of Kir4.1 function inhibits the function of the Na^+-K^+-ATPase via loss of potassium recycling, reduces basolateral chloride reabsorption by rendering the membrane potential (E_m) less negative, and thereby inhibits both apical Na^+ and Cl^- reabsorption by NCCT and Mg^{2+} reabsorption because of a less negative membrane potential. The resulting renal salt loss activates the renin-angiotensin-aldosterone system. Increased amounts of Na^+ and Cl^- are delivered to the cortical collecting duct, where aldosterone dependent Na^+ reabsoption via ENaC is coupled to K^+ and H^+ secretion (see *Discussion*), thus accounting for the hypokalemic alkalosis observed.

immunolocalized in the kidney. In contrast to the apical K^+ channels (e.g., *KCNJ1* encoding ROMK and *KCNMA1* encoding Maxi-K) that mediate K^+ secretion in the distal nephron, Kir4.1 localizes to the basolateral membranes of epithelia of the distal convoluted tubule, connecting tubule, and initial collecting tubule (29). Weak immunoreactivity in the thick ascending limb of Henle has also been described (12). Our patients with *KCNJ10* deficiency display hypokalemia, metabolic alkalosis, hypomagnesemia and, where studied, elevated levels of renin and aldosterone. The high renin and aldosterone, along with normal blood pressure, hypokalemia, and metabolic alkalosis strongly point to salt wasting as an incipient event in the renal features, and the reports of salt craving, polyuria, and enuresis are consistent with this. Moreover, these patients have elevated urinary sodium/creatinine ratios in the range seen in patients with Gitelman syndrome (see Table 1) (30). Loss of *KCNJ10* function can result in salt wasting by impairing the activity of the Na^+-K^+-ATPase. The Na^+-K^+-ATPase is on the basolateral membrane, and its activity is required for Na^+ reabsorption, pumping Na^+ out of epithelia and K^+ in against their electrochemical potentials. Because very large amounts of filtered Na^+ must be reabsorbed by renal epithelia, the K^+ that enters the epithelial cell must be recycled to the interstitium by basolateral K^+ channels to allow continued Na^+ reabsorption. Without this mechanism, the Na^+-K^+-ATPase could be inhibited and the potential across the basolateral membrane diminished. This diminished negative intracellular potential will also attenuate the electrical gradient for the efflux of Cl^- (Fig. 4*B*). The combined effects will produce impaired Na-Cl reabsorption.

Because much is known about the consequences of inhibition of salt reabsorption in different nephron segments (31, 32), we can make inferences about where the effects of *KCNJ10* deficiency are impairing salt reabsorption. The only site at which inhibition of salt reabsorption produces hypomagnesemia with reduced urinary calcium is the distal convoluted tubule. In contrast, loss of salt reabsorption in the thick ascending limb produces marked hypercalciuria and little hypomagnesemia (5), while loss of ENaC activity in the collecting duct produces hyperkalemia and acidosis rather than hypokalemia and alkalosis (33). We consequently believe it is highly likely that impaired salt reabsorption in the DCT plays a prominent role in this syndrome. Because epithelial cells of the DCT have the greatest per-cell Na^+ reabsorption and energy demand (34), it is possible that sodium pump activity in other nephron segments is also affected, but that the effect in the DCT predominates.

These considerations suggest an integrated model in which loss of Kir4.1 activity impairs salt reabsorption in the distal convoluted tubule (see Fig. 4). Because salt reabsorption in the DCT comprises ≈7% of the filtered load, loss of salt reabsorption here induces salt wasting, which activates the renin-angiotensin system, increasing Na^+ reabsorption by the ENaC in the connecting tubule and collecting duct. This increases the electrical driving force for both K^+ and H^+ secretion, resulting in hypokalemia and metabolic alkalosis. As described above, loss of salt reabsorption in the DCT is also known to produce hypocalciuria and hypomagnesemia. While these renal electrolyte defects seem relatively mild, it is noteworthy that 2 siblings with this syndrome have died in the setting of diarrheal or other intercurrent infections, suggesting impaired ability to defend volume homeostasis under stress.

Little is known about the genes that underlie the most prevalent forms of epilepsy. In the last decade, gene defects have been identified that cause rare Mendelian forms of idiopathic epilepsy syndromes, and most of these genes encode ion channels, consistent with their role in maintaining membrane potential and regulating neuronal excitability (11). It will be interesting to determine the prevalence of epilepsy caused by mutations in the *KCNJ10* gene. In addition to the characteristic neurological features (developmental delay, ataxia, and hearing impairment), a simple blood test might help to screen for such patients, as all patients in this report presented with significant hypokalemia and hypomagnesemia.

These human findings raise the possibility that Kir4.1 could be a useful target for pharmacologic manipulation. Similar to the recently developed anticonvulsant drug retigabine, which opens KCNQ2/3 channels (35), a Kir4.1 activator might have anticonvulsant effects; nonetheless, the expression of Kir4.1 in several tissues raises the question of whether there might be pleiotropic effects that could limit utility.

In summary, our data define a unique autosomal, recessive syndrome characterized by seizures, sensorineural deafness, ataxia, mental retardation, and electrolyte imbalance (hypokalemic alkalosis and hypomagnesemia), and demonstrate that it is caused by mutations in *KCNJ10*. We propose the acronym SeSAME to refer to this disorder.

Materials and Methods

Patient Recruitment and DNA Preparation. The study protocol was approved by the Yale Human Investigation Committee. Consent for participation was obtained in accordance with Institutional Review Board standards. Patients were referred for studies of hypokalemic salt-losing nephropathies, and kindreds were chosen for further analysis by the presence of seizures, ataxia, and hearing impairment. Genomic DNA was prepared from venous blood of kindred members by standard procedures.

Genotyping. The samples were genotyped on the Illumina Human CNV370-Duo (for 441–1) and Illumina Human 610-Quad (for 404–1, 632–1, and 632–2) beadchips at the W.M. Keck Facility at Yale University. Sample processing and labeling were performed using the manufacturer's instructions. Mean call rate of the 4 samples was 99.50%.

Mapping Homozygous and IBD Intervals. Because the genotype data from 441–1 and 404–1 were originated from different arrays, the data were compared to generate a list of 346,073 shared SNPs to be subjected to homozygosity mapping. Analysis of homozygous segments across 22 autosomes was performed using the ''Runs of homozygosity'' tool implemented in PLINK (v1.05). A fixed threshold of 200 consecutive SNPs and 2 Mb in length was selected, and 1 heterozygous SNP within a segment was allowed.

To check the IBD shared regions between the affected siblings, the genotype data from 632–1 and 632–2 were directly compared. Missing calls were

discarded. Fixed thresholds of 200 consecutive SNPs and 1 Mb in length were used to call IBD segments.

DNA Sequencing. A primer pair (KCNJ10_F: 5′-CATGGGGTGAGGGTTAGGAG-3′ and KCNJ10_R: 5′-GGGAGTGGAGGATGGGTG-3′) was used to amplify the coding exon of *KCNJ10* using as a template genomic DNA of disease family members or controls. PCR generated a product with a size of 1,325 bp. Products were analyzed via gel electrophoresis, and purified amplicons were sequenced using the KCNJ10_F, KCNJ10_R, KCNJ10MF (5′-CGGGCTGAGACCATTCGTTTC-3′) and KCNJ10MR (5′-AGGCTTTTGCGCATATTGGAAC-3′) primers. Disease-causing mutations were confirmed by at least 2 independent sequences from different primers. In addition, in the 2 kindreds in which affected subjects were apparent compound heterozygotes, the coding region was amplified and cloned using the TOPO TA Cloning Kit (Invitrogen), and independent clones from each patient were sequenced to determine whether the identified mutations were *in cis* or *trans*.

Orthologs and Paralogs. Full-length orthologous and paralogous protein sequences from vertebrate and invertebrate species (including rodents, bird, fish, and fly) were extracted from GenBank. Orthologs were confirmed based on database identity of annotation or in a BLAST of the protein sequence against the human protein sequence, with the requirement that human *KCNJ10* be the top hit. If an ortholog could not be identified, a paralog was studied. Protein sequences were aligned using the ClustalW algorithm. GenBank accession numbers were: NP_002232.2 (human KCNJ10), NP_001034573.1 (mouse KCNJ10), XP_425554.2 (chicken paralog), NP_001072312.1 (frog KCNJ10), XP_001342993.1 (zebrafish ortholog), and NP_001097884.1 (fly paralog).

ACKNOWLEDGMENTS. We thank the members of the families studied and their physicians for their invaluable contribution to this project. We thank Dr. Sally-Anne Hulton (The Birmingham Children's Hospital) and the Department of Paediatrics, Klinikum Worms, Germany for referral of patients 327–1 and 404–1, respectively; Dr. Willem Proesmans (University Hospital Gasthuisberg, Belgium) for advice in the evaluation of patient 441–1; Dr. Gerhard Giebisch (Yale University School of Medicine), Dr. Stephen Waxman (Department of Neurology, Yale University School of Medicine), and members of the Lifton, State and Günel laboratories (Department of Genetics, Yale University School of Medicine) for helpful discussions. This study was supported by the Leducq Transatlantic Network in Hypertension and the Yale O'Brien Center.

1. Karet FE, et al. (1999) Mutations in the gene encoding B1 subunit of H+-ATPase cause renal tubular acidosis with sensorineural deafness. *Nat Genet* 21:84–90.
2. Birkenhager R, et al. (2001) Mutation of BSND causes Bartter syndrome with sensorineural deafness and kidney failure. *Nat Genet* 29:310–314.
3. Hansson JH, et al. (1995) Hypertension caused by a truncated epithelial sodium channel gamma subunit: genetic heterogeneity of Liddle syndrome. *Nat Genet* 11:76–82.
4. Simon DB, et al. (1997) Mutations in the chloride channel gene, *CLCNKB*, cause Bartter's syndrome type III. *Nat Genet* 17:171–178.
5. Simon DB, et al. (1996) Bartter's syndrome, hypokalaemic alkalosis with hypercalciuria, is caused by mutations in the Na-K-2Cl cotransporter NKCC2. *Nat Genet* 13:183–188.
6. Simon DB, et al. (1996) Genetic heterogeneity of Bartter's syndrome revealed by mutations in the K+ channel, ROMK. *Nat Genet* 14:152–156.
7. Simon DB, et al. (1996) Gitelman's variant of Bartter's syndrome, inherited hypokalaemic alkalosis, is caused by mutations in the thiazide-sensitive Na-Cl cotransporter. *Nat Genet* 12:24–30.
8. Biervert C, et al. (1998) A potassium channel mutation in neonatal human epilepsy. *Science* 279:403–406.
9. Charlier C, et al. (1998) A pore mutation in a novel KQT-like potassium channel gene in an idiopathic epilepsy family. *Nat Genet* 18:53–55.
10. Heron SE, et al. (2002) Sodium-channel defects in benign familial neonatal-infantile seizures. *Lancet* 360:851–852.
11. Weber YG, Lerche H (2008) Genetic mechanisms in idiopathic epilepsies. *Dev Med Child Neurol* 50:648–654.
12. Tanemoto M, Abe T, Onogawa T, Ito S (2004) PDZ binding motif-dependent localization of K+ channel on the basolateral side in distal tubules. *Am J Physiol Renal Physiol* 287:F1148–F1153.
13. Lopes CM, et al. (2002) Alterations in conserved Kir channel-PIP2 interactions underlie channelopathies. *Neuron* 34:933–944.
14. Schulte U, et al. (1998) pH-dependent gating of ROMK (Kir1.1) channels involves conformational changes in both N and C termini. *J Biol Chem* 273:34575–34579.
15. Rapedius M, et al. (2007) Control of pH and PIP_2 gating in heteromeric Kir4.1/Kir5.1 channels by H-Bonding at the helix-bundle crossing. *Channels* (*Austin*) 1:327–330.
16. Nishida M, Cadene M, Chait BT, MacKinnon R (2007) Crystal structure of a Kir3.1-prokaryotic Kir channel chimera. *EMBO J* 26:4005–4015.
17. Ji W, et al. (2008) Rare independent mutations in renal salt handling genes contribute to blood pressure variation. *Nat Genet* 40:592–599.
18. Lachheb S, et al. (2008) Kir4.1/Kir5.1 channel forms the major K+ channel in the basolateral membrane of mouse renal collecting duct principal cells. *Am J Physiol Renal Physiol* 294:F1398–F1407.
19. Lourdel S, et al. (2002) An inward rectifier K(+) channel at the basolateral membrane of the mouse distal convoluted tubule: similarities with Kir4-Kir5.1 heteromeric channels. *J Physiol* 538:391–404.
20. Djukic B, et al. (2007) Conditional knock-out of Kir4.1 leads to glial membrane depolarization, inhibition of potassium and glutamate uptake, and enhanced short-term synaptic potentiation. *J Neurosci* 27:11354–11365.
21. Kofuji P, et al. (2000) Genetic inactivation of an inwardly rectifying potassium channel (Kir4.1 subunit) in mice: phenotypic impact in retina. *J Neurosci* 20:5733–5740.
22. Neusch C, et al. (2001) Kir4.1 potassium channel subunit is crucial for oligodendrocyte development and in vivo myelination. *J Neurosci* 21:5429–5438.
23. Rozengurt N, et al. (2003) Time course of inner ear degeneration and deafness in mice lacking the Kir4.1 potassium channel subunit. *Hear Res* 177:71–80.
24. Takumi T, et al. (1995) A novel ATP-dependent inward rectifier potassium channel expressed predominantly in glial cells. *J Biol Chem* 270:16339–16346.
25. Kofuji P, Newman EA (2004) Potassium buffering in the central nervous system. *Neuroscience* 129:1045–1056.
26. Buono RJ, et al. (2004) Association between variation in the human KCNJ10 potassium ion channel gene and seizure susceptibility. *Epilepsy Res* 58:175–183.
27. Ando M, Takeuchi S (1999) Immunological identification of an inward rectifier K+ channel (Kir4.1) in the intermediate cell (melanocyte) of the cochlear stria vascularis of gerbils and rats. *Cell Tissue Res* 298:179–183.
28. Hibino H, et al. (1999) Expression of an inwardly rectifying K(+) channel, Kir4.1, in satellite cells of rat cochlear ganglia. *Am J Physiol* 277:C638–C644.
29. Ito M, et al. (1996) Immunolocalization of an inwardly rectifying K+ channel, K(AB)-2 (Kir4.1), in the basolateral membrane of renal distal tubular epithelia. *FEBS Lett* 388:11–15.
30. Cruz DN, et al. (2001) Mutations in the Na-Cl cotransporter reduce blood pressure in humans. *Hypertension* 37:1458–1464.
31. Nijenhuis T, et al. (2005) Enhanced passive Ca2+ reabsorption and reduced Mg2+ channel abundance explains thiazide-induced hypocalciuria and hypomagnesemia. *J Clin Invest* 115:1651–1658.
32. Schultheis PJ, et al. (1998) Phenotype resembling Gitelman's syndrome in mice lacking the apical Na+-Cl- cotransporter of the distal convoluted tubule. *J Biol Chem* 273:29150–29155.
33. Chang SS, et al. (1996) Mutations in subunits of the epithelial sodium channel cause salt wasting with hyperkalaemic acidosis, pseudohypoaldosteronism type 1. *Nat Genet* 12:248–253.
34. Reilly RF, Ellison DH (2000) Mammalian distal tubule: physiology, pathophysiology, and molecular anatomy. *Physiol Rev* 80:277–313.
35. Rundfeldt C, Netzer R (2000) The novel anticonvulsant retigabine activates M-currents in Chinese hamster ovary-cells tranfected with human KCNQ2/3 subunits. *Neurosci Lett* 282:73–76.
36. Halperin ML, Kamel KS (1998) Potassium. *Lancet* 352:135–140.